ELSEVIER

Journal of Nuclear Materials 266–269 (1999) 1191–1196

journal of nuclear materials

Plasma characteristics near the X-point in W-shaped divertor of JT-60U

S. Sakurai *, N. Asakura, N. Hosogane, K. Itami, M. Shimada, O. Naito

Japan Atomic Energy Research Institute, Naka Fusion Research Establishment, Naki-machi, Naka-gun, Ibaraki 311-01, Japan

Abstract

A reciprocating Langmuir probe was installed below the X-point of W-shaped divertor in JT-60U. Plasma profiles were measured from the outer divertor nose to the X-point. A large peak was observed in the density profile near the X-point as the main plasma density exceeded about 60% of MARFE onset density. The electron density at the peak exceeded the average density of the main plasma. The difference in electron temperature between the X-point and the outer target was smaller at the separatrix than outside the separatrix. The electron temperature near the separatrix decreased rapidly from 60 to 20 eV as the density peak increased. The electron temperature profile became flat and decreased down to ~10 eV during a MARFE.

Keywords: Divertor plasma; Probe; X-point

1. Introduction

Formation of a cold, dense and radiative divertor is essential to reduce the heat flux to the divertor target plate. A reciprocating Langmuir probe system was installed below the X-point of the W-shaped divertor in JT-60U [1,2] to investigate the cold and dense plasma formation predicted by numerical results [2,3]. An experimental database of decay lengths of heat and particle fluxes near the divertor nose is important for designing the baffle plate of the closed divertor. Fast reciprocating Langmuir probes have been installed in many tokamaks [4–7], and have provided profiles of the local electron temperature and density with high spatial resolution. The high spatial resolution is essential to investigate the mechanism of divertor detachment and MARFE formation, which are related to local phenomena near the X-point.

In this paper, we show divertor plasma characteristics measured with Langmuir probes. The temperature and pressure differences between the X-point and the target plates are discussed. The density and temperature decay lengths near the X-point are shown. Estimation of ion flow velocity near the X-point is discussed.

2. Experimental set-up

The divertor reciprocating Langmuir probe system and related diagnostics are shown in Fig. 1. Plasma profiles were measured from the outer divertor nose to the X-point. The duration of insertion and retraction is 1 s for the stroke of 250 mm reciprocating.

The probe head and electrodes are made of Carbon Fiber Composites (CFC) and the electrodes are insulated by ceramics. Electron temperature and ion flux at the upstream (toward the main plasma) and downstream (toward the target plate) sides of the probe can be measured simultaneously by using two sets of double probes facing upstream and downstream.

The plasma shape, position, density and heating power were kept constant during measurement. After the probe insertion, the strike point was swept by about 4 cm in 1.5 s to obtain a plasma profile at the target plate.

* Corresponding author. Tel.: +81-619 455 4477; fax: +81-619 455 4156; e-mail: sakuarais@fusion.naka.jaeri.go.jp

0022-3115/99/$ – see front matter
PII: S0022-3115(98)00635-7

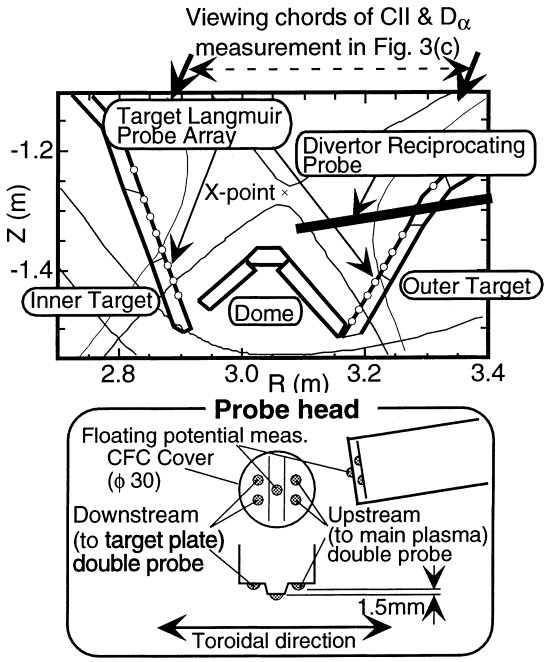

Fig. 1. Experimental set-up of related diagnostics and configuration of the head of divertor reciprocating probe.

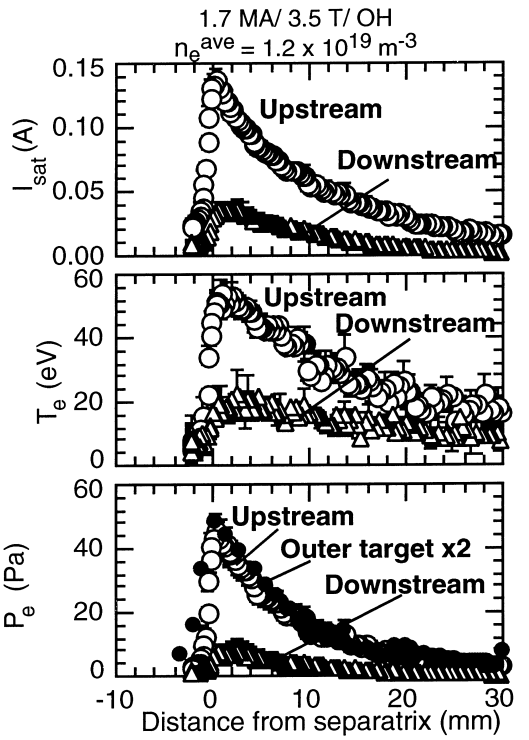

Fig. 2. Typical measurements of the divertor reciprocating probe. Ion saturation current I_{sat} and electron temperature T_e at both sides of the probe head are shown in the top and middle box. Electron pressures P_e ($=n_eT_e$) at both sides and at the outer target ($=n_eT_e \times 2$) are shown in the bottom box. All measurements are mapped on the mid-plane radius.

3. Results

3.1. Plasma profiles near the X-point

Typical results of ohmic heated discharges (1.7 MA, 3.5 T) are shown here. The plasma equilibrium for this study was fixed as shown in Fig. 1(a) and the X-point position 6 cm above the path of probe reciprocation. Profiles of ion saturation current I_{sat} and electron temperature T_e at the upstream and downstream sides are shown in Fig. 2(a) and (b). I_{sat} at the upstream side was by a factor of 3–8 times larger than at the downstream side, and T_e at the upstream side was about twice as large as at the downstream side. Measurements at the upstream side were used for comparison with those by target probe arrays because of good agreement in electron pressure profile at the X-point and the outer target in low density discharges as shown in Fig. 2(c).

A large peak was observed in the electron density profile near the X-point when the line averaged main density $n_e^{ave.}$ exceeded about 60% of MARFE onset density (2.4×10^{19} m^{-3}) as shown in the top box of Fig. 3(a) and (b). A similar observation was also made near the X-point in ASDEX-U [7] and at the target in Alcator C-Mod [8] and JET [9] in the high recycling divertor plasma. The electron density n_e at the peak exceeded the line averaged density of main plasma. T_e near the separatrix decreased from 60 to 20 eV at the density peak. During a MARFE, the density peak was reduced and the density profile slightly broadened. T_e was reduced down to ≈10 eV and the temperature profile became flat.

3.2. Comparison with measurements by target Langmuir probe arrays

The profiles of n_e and T_e at X-point and target plates are shown in Fig. 3(a) and (b) respectively, and they are compared in three cases: at low density ($n_e^{ave.} = 1.2 \times 10^{19}$ m^{-3}), at high density ($1.7–1.9 \times 10^{19}$ m^{-3}) and during the MARFE (2.4×10^{19} m^{-3}). The CII and D_α emission at the divertor region and the ion saturation current I_{sat} at the inner and outer target are shown in Fig. 3(c). The particle recycling increases as the density increases. The carbon impurity near the X-point increases and I_{sat} to the inner target is reduced during a MARFE.

n_e at the inner target is larger than those at the outer target and X-point, and T_e at the outer target and X-point (≈60 eV) were higher than at the inner target (≈20 eV) at low density.

At high density (1.9×10^{19} m^{-3}), the n_e profile at the X-point agrees well with those at the inner and outer

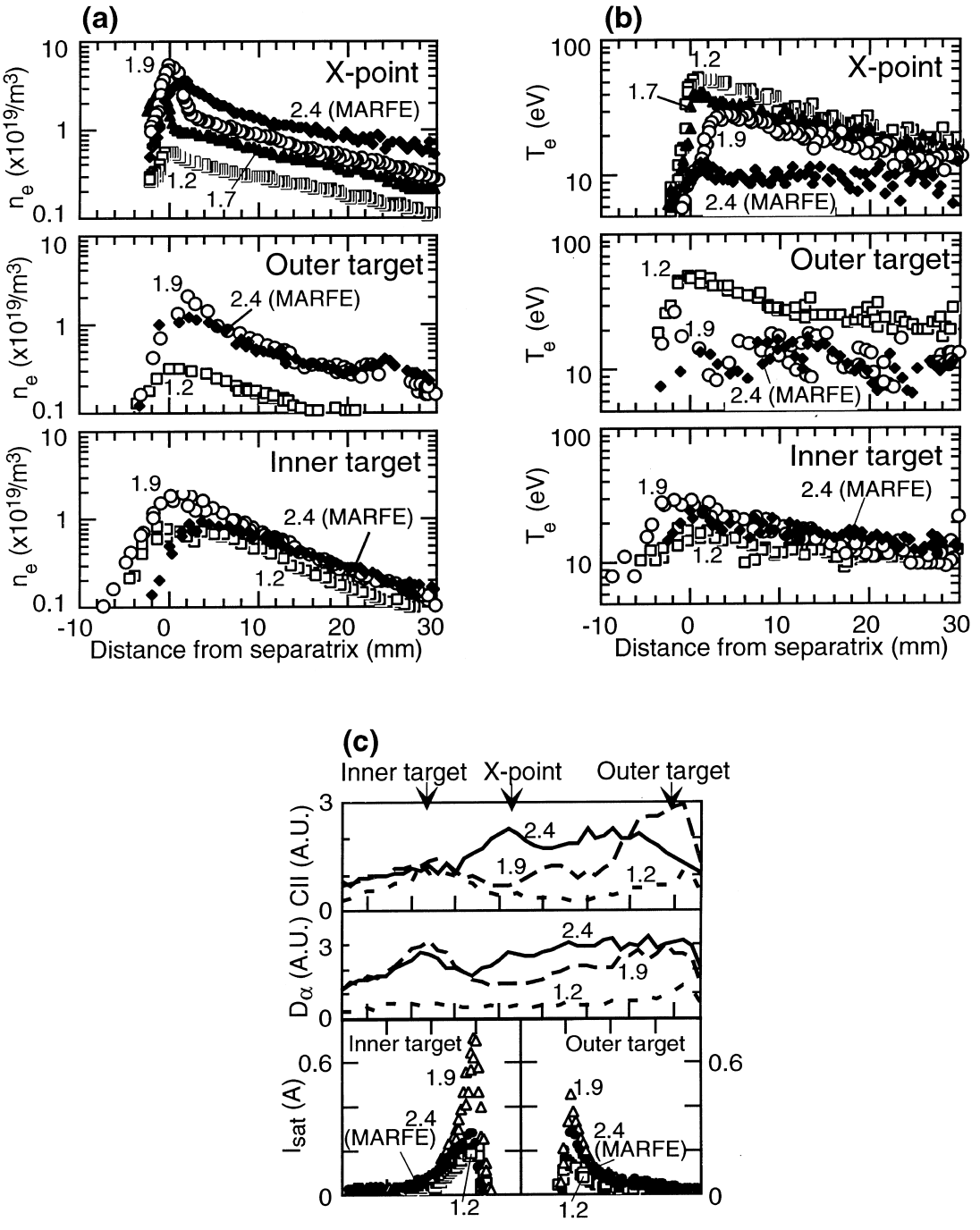

Fig. 3. Dependence of (a) density and (b) temperature profiles at three positions (X-point, inner and outer target) and (c) CII, D_α emission and ion saturation current profiles at divertor on main plasma density in OH discharges with $I_p = 1.7$ MA and $B_t = 3.5$ T. Line averaged main densities (10^{19} m^{-3}) are shown in figures.

targets except for the density peak near the separatrix. T_e at the outer target decreases to 10–20 eV. At the X-point, T_e near the separatrix decreases similar to that at the outer target (10–20 eV). On the other hand, T_e at the X-point remains higher (20–30 eV) at the outside (2–15 mm) of the separatrix.

n_e profile at the X-point broadens and exceeds those at the targets during a MARFE. T_e decreases down to

≈10 eV at the X-point and outer target during a MARFE.

3.3. Pressure balance between the X-point and the target

At low density (1.2×10^{19} m^{-3}), the electron pressure P_e profile at the X-point agrees well with those at both targets as shown in Fig. 4(a). The reciprocating probe-derived pressure is compared with 2 × the target probe-derived pressures, because the sonic conditions are assumed in calculating the pressure at the target [8].

During a MARFE (2.4×10^{19} m^{-3}), the I_{sat} shown in Fig. 3(c) and P_e shown in Fig. 4(b) and (c) decrease at the separatrix in comparison to those at high density (1.9×10^{19} m^{-3}). Furthermore, a small moment loss between X-point and the outer target is observed as shown in Fig. 4(c). Therefore, it seems that the weak partial detachment was obtained at both targets during a MARFE. There is some uncertainty in this argument, e.g., there is a higher P_e at the inner target at high density (1.9×10^{19} m^{-3}) and the measured T_e (10–20 eV) is too high to enhance momentum loss. This will be discussed in Section 4.

The electron pressure at the X-point also decreases during a MARFE. This suggests that the power and momentum are dispersed above the measured position (≈6 cm below the X-point).

3.4. Scrape-off layer decay lengths near the X-point

The e-folding length of electron density and temperature profiles, λ_{n_e} and λ_{T_e}, were measured at the X-point. Exponential fitting was applied between 10 and 30 mm outside the separatrix to avoid the peak in n_e profile and the reduction in T_e profile near the separatrix. The results are shown in Fig. 5 as a function of n_e^{ave}. Values of λ_{n_e} (≈20 mm) and λ_{T_e} (≈30 mm) are independent of the main density and heating method (OH or low power NB) under the attached condition. λ_{T_e} increased rapidly during a MARFE, because the electron temperature profile became very flat as shown in Fig. 3(b). The same result was observed at the mid-plane [10].

4. Discussion

At high density (1.9×10^{19} m^{-3}), a large peak in n_e profile is formed near the X-point. T_e near the separatrix at the X-point decreases similar to that at the outer target. This suggests that particle recycling and radiation loss are enhanced along the separatrix, which were expected from simulations as a W-shape (inclined target) effect.

The electron density at the X-point is larger than at the outer target not only near the separatrix but also radially away from the separatrix during a MARFE.

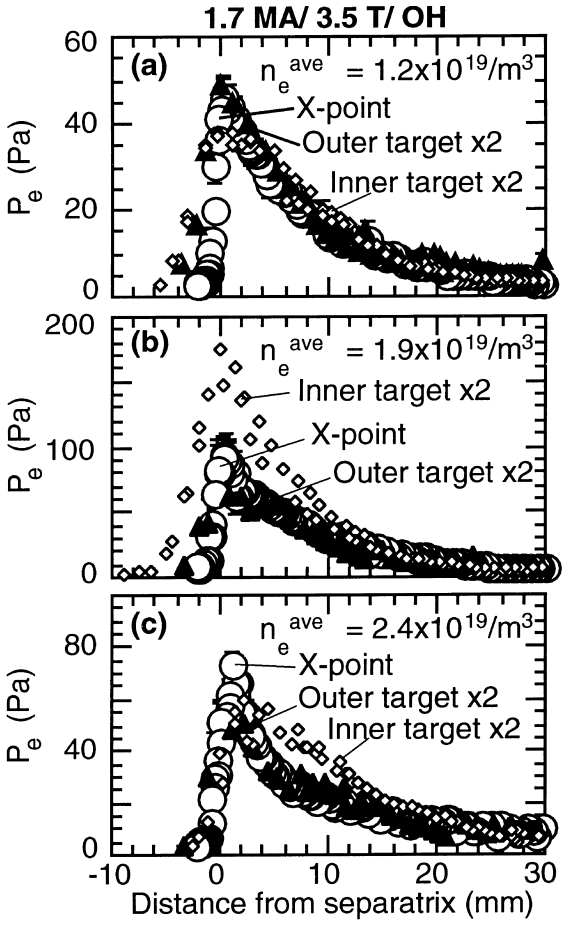

Fig. 4. Electron pressure P_e balance between the X-point and both target plates and its dependence on main plasma density. All measurements are mapped on the mid-plane radius.

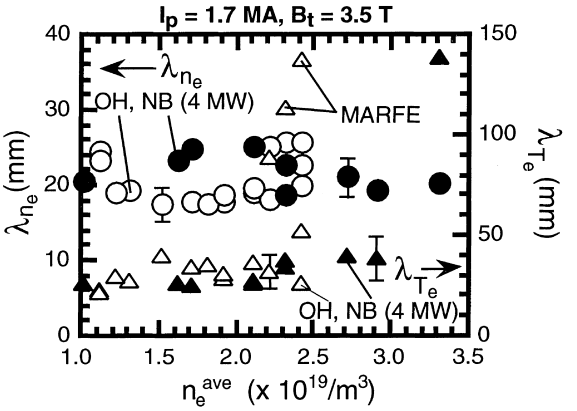

Fig. 5. Dependence of radial decay lengths of electron density λ_{n_e} and temperature λ_{T_e} on line averaged main plasma density. Open and closed symbols show OH and NB (4 MW) discharges respectively.

This may be due to the impurity ion concentration near the X-point and neutrals penetrating far from the target as shown in the emission profiles in Fig. 3(c).

P_e ($=n_e \times T_e$) at high density (1.9×10^{19} m^{-3}) at the inner target seems higher than those at the outer target and X-point, since T_e at the inner target does not decrease inspite of the increment of particle recycling shown in Fig. 3(c) as D_α emission and I_{sat}. Measured electron temperatures (10–20 eV) at the X-point and targets seem to be too high to enhance a momentum loss. There are some possibilities of overestimation in electron temperature of the probe measurement in magnetic field [11,12]. A single Langmuir probe acts as an asymmetric double probe in a strong magnetic field. Furthermore, a small perturbation of high energy tail of the electron distribution can introduce a significant error in the derived T_e, since Langmuir probes only measure this tail.

Ion saturation current at the upstream I_{sat}^{up} and downstream side I_{sat}^{down} were measured as shown in Fig. 2. Under the experimental conditions for this study, the connection length L_c between the X-point and the outer target along the magnetic field line (1–5 m) is comparable to the probe collection length [13] defined as $C_s\ \Delta^2/D_{perp}$, where C_s is the ion sound velocity, Δ is the dimension of probe head ($\geqslant 1.5$ mm) as shown in Fig. 1, D_{perp} is the cross field diffusion coefficient. Therefore, the measured $I_{sat}^{up}/I_{sat}^{down}$ ratio is much larger than expected from the Mach probe theories [13,14].

To estimate the effect of the short connection length on the measured $I_{sat}^{up}/I_{sat}^{down}$ ratio, the plasma density reduction in the flux tube between the probe electrodes and targets plate was roughly evaluated by the limiter terminated SOL model. The radial decay length in the flux tube λ_n is $(D_{perp} \times L_c/C_s)^{1/2}$. Therefore, the effect on the measured $I_{sat}^{up}/I_{sat}^{down}$ ratio is the ratio of $\exp(-\Delta/\lambda_n)$ at upstream and downstream sides. This effect depends on not only the connection length but also the plasma conditions at the upstream and downstream sides. This effect is less than a factor of 2–3 under the experimental conditions even if the temperature and cross field transport change by a factor of 2–3 between the upstream and downstream sides. Although there is some uncertainty in applying this estimation to the MARFE and detachment, the measured $I_{sat}^{up}/I_{sat}^{down}$ ratio is shown as a qualitative index of the plasma flow in this paper.

The profiles of $I_{sat}^{up}/I_{sat}^{down}$ ratio are shown in Fig. 6. The ratio near the X-point exceeds 10 as n_e^{ave} increases. The ratio decreases somewhat at the separatrix and increases outside the separatrix during a MARFE. In discharges with reversed plasma current and toroidal field (ion grad-B drift direction is opposite to the target), the flow velocity near the separatrix remained small and increased outside the separatrix. These results seem to be inconsistent with the effect of ion grad-B drift direction on the global in–out flux asymmetry; the flux towards the inner target is larger with the normal I_p and B_t direction and

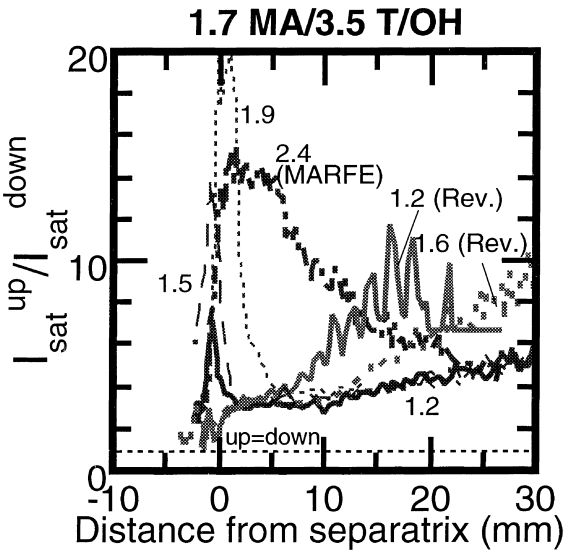

Fig. 6. Profiles of the ratio of ion saturation current $I_{sat}^{up}/I_{sat}^{down}$ at the X-point. The line averaged main plasma density ($\times 10^{19}$ m^{-3}) and the direction of plasma current and toroidal field are shown. All measurements are mapped on the mid-plane radius.

becomes symmetric with reversed I_p and B_t. On the other hand, the plasma flow measurement by the mid-plane reciprocating probe shows that the flow near the mid-plane is directed upstream with the normal I_p and B_t direction and downstream with reversed I_p and B_t.

5. Summary

The divertor reciprocating Langmuir probe system was installed at the outer divertor chamber of the W-shaped divertor in JT-60U. The plasma profiles were measured from the outer divertor nose to the X-point.

A large peak was observed in the density profile near the X-point as n_e^{ave} exceeded about 60% of the MARFE onset density; n_e at the peak exceeds the average density of main plasma. T_e near the separatrix at the X-point and outer target decreases rapidly from 60 eV to 20 eV as the density peak grows. The T_e profile became flat and decreased down to ≈10 eV during a MARFE.

Values of λ_{n_e} (≈20 mm) and λ_{T_e} (≈30 mm) at the X-point are independent of the main density and heating method (OH or low power NB) except for the MARFE case. λ_{T_e} increased rapidly during a MARFE similarly at the mid-plane.

Although there is some uncertainty due to the short connection length and plasma conditions, the measured $I_{sat}^{up}/I_{sat}^{down}$ ratio can be used as a qualitative index of the plasma flow. In discharges with reversed plasma current and toroidal field (ion grad-B drift direction is opposite to that of the target), the flow velocity near the

separatrix remained small and increased outside the separatrix in comparison to those with normal I_p and B_t direction.

Acknowledgements

The authors would like to thank the members of the Japan Atomic Energy Research Institute who have contributed to the JT-60U project.

References

[1] S. Sakurai et al., Fusion Tech. 1996 (1997) 471.
[2] N. Hosogane et al., 16th IAEA Fusion Energy Conf., Montreal, 1996, IAEA-CN-64/GP-11.
[3] S. Tsuji et al., J. Nucl. Mater. 220–222 (1995) 400.
[4] T.L. Rhodes et al., Rev. Sci. Instrum. 61 (1990) 3001.
[5] J.G. Watkins et al., Rev. Sci. Instrum. 63 (1992) 4728.
[6] N. Asakura et al., Rev. Sci. Instrum. 66 (1995) 5428.
[7] C.S. Pitcher et al., J. Nucl. Mater. 220–222 (1995) 213.
[8] B. LaBombard et al., Phys. Plasmas 2 (1995) 2242.
[9] R.D. Monk et al., J. Nucl. Mater. 220–222 (1995) 612.
[10] N. Asakura et al., J. Nucl. Mater. 241–243 (1997) 559.
[11] K. Günter et al., J. Nucl. Mater. 176&177 (1990) 236.
[12] P.C. Stangeby, Plasma Phys. Control Fusion 37 (1995) 1031.
[13] P.C. Stangeby, Phys. Fluids. 27 (1984) 2699.
[14] I.H. Hutchinson, Phys. Rev. A 37 (1988) 4358.